

# Patterned Growth of ZnO Nanowire Arrays on Zinc Foil by Thermal Oxidation

Farid Jamali Sheini, Dilip S. Joag, Mahendra A. More

**Abstract**—A simple approach is demonstrated for growing large scale, nearly vertically aligned ZnO nanowire arrays by thermal oxidation method. To reveal effect of temperature on growth and physical properties of the ZnO nanowires, gold coated zinc substrates were annealed at 300 °C and 400 °C for 4 hours duration in air. X-ray diffraction patterns of annealed samples indicated a set of well defined diffraction peaks, indexed to the wurtzite hexagonal phase of ZnO. The scanning electron microscopy studies show formation of ZnO nanowires having length of several microns and average of diameter less than 500 nm. It is found that the areal density of wires is relatively higher, when the annealing is carried out at higher temperature i.e. at 400°C. From the field emission studies, the values of the turn-on and threshold field, required to draw emission current density of 10  $\mu\text{A}/\text{cm}^2$  and 100  $\mu\text{A}/\text{cm}^2$  are observed to be 1.2 V/ $\mu\text{m}$  and 1.7 V/ $\mu\text{m}$  for the samples annealed at 300 °C and 2.9 V/ $\mu\text{m}$  and 3.7 V/ $\mu\text{m}$  for that annealed at 400 °C, respectively. The field emission current stability, investigated over duration of more than 2 hours at the preset value of 1  $\mu\text{A}$ , is found to be fairly good in both cases. The simplicity of the synthesis route coupled with the promising field emission properties offer unprecedented advantage for the use of ZnO field emitters for high current density applications.

**Keywords**—ZnO, Nanowires, Thermal oxidation, Field Emission.

## I. INTRODUCTION

RECENTLY, many efforts have been focused to fabricate various one-dimensional (1-D) nanostructures, due to their novel physical and chemical properties and promising applications in diversified areas. As an important metal oxide, ZnO nanostructures have attracted much attention of the researchers, since they are considered as potential candidates for gas sensors [1], laser [2] and nanogenerator (piezoelectricity) [3]. In addition, ZnO nanovariants such as, nanoneedles, nanowires, nanotubes, terapopds, nanobets, etc., have been investigated from the field emission based application point of view [4-8]. Synthesis of ZnO nanostructures have been carried out by various methods, based on vapour transport process, which are categorized into two groups viz, the catalyst free vapor-solid (VS) process and the catalyst assisted vapor-liquid-solid

(VLS) process. It has been observed that the VS method has limited control on the location, growth direction and even on the size of the nanostructures, as contrast to the VLS route [9, 10]. The VLS synthesis route deals with the growth of the nanostructure from a metal alloying droplet [11, 12] and has been widely used to illustrate growth of various semiconducting nanostructures above the eutectic point of the alloy droplet.

In the context of field emission based applications, as observed from the literature, 1-D ZnO nanostructures exhibit excellent emission competence at par with the carbon nanotubes. In order to envisage field emission based devices, well defined array of nanostructures is a pre-requisite. There have been attempts to fabricate an array of 1-D ZnO nanostructures and study their field emission behaviour [13-14]. In most of these studies, silicon has been used as substrate for growth of the nanostructures arrays. Field emission, although being surface sensitive phenomenon, in case of multi-emitters (an array of nanostructures) grown on a substrate, the substrate properties, in particular, the electrical conductivity, plays an important role in deciding their field emission characteristics. In this paper, we report fabrication of an array of aligned ZnO nanostructures, grown on zinc substrate by a simple thermal oxidation route and its field emission characteristics. Effect of the annealing temperature on the field emission properties has been investigated. From the field emission results values of the turn-on field and threshold field, corresponding to emission current density of 10  $\mu\text{A}/\text{cm}^2$  and 100  $\mu\text{A}/\text{cm}^2$  are observed to be 1.2 V/ $\mu\text{m}$  and 1.7 V/ $\mu\text{m}$  for the sample annealed at 300 °C and 2.9 V/ $\mu\text{m}$  and 3.7 V/ $\mu\text{m}$  for the annealed at 400 °C, respectively, which are comparable to those reported in the literature.

## II. EXPERIMENTAL DETAILS

The ZnO nanostructures were prepared by annealing of zinc foil coated with a thin layer of gold. The Zn foils (99.99%, Alfa Aesar) used as substrates, were ultrasonically cleaned in acetone and methanol for 10 minutes in each solvent. A thin layer of gold, (thickness  $\sim$  60 nm), was deposited onto the substrates by vacuum evaporation method at a base pressure of  $1 \times 10^{-5}$  mbar. The gold layer thickness was measured using Taly step method (Taylor-Hobson). Using Uv photolithography, a 'square' pattern of gold islands ( $400 \times 400 \mu\text{m}^2$ ) separated by  $400 \mu\text{m}$  was generated on the substrate. In order to reveal the effect of temperature on growth and physical properties of the ZnO nanostructures, the patterned substrates were annealed at 300 °C and 400 °C for 4 hours duration in air, in separate experiments. The annealing was carried out at the ambient pressure in a laboratory furnace.

Farid Jamali-Sheini, Department of Physics, Islamic Azad University, Ahwaz Branch, Ahwaz, Iran. Ph. +98 - 611 - 3348420 - 24, Fax. +98 - 611 - 3329200 e-mail: faridjamali@iauhvaz.ac.ir

Dilip S. Joag, Mahendra A. More, Center for Advanced Studies in Materials Science and Condensed Matter Physics, Department of Physics, University of Pune, Pune - 411007, India. e-mail (D.S. Joag): dsj@physics.unipune.ac.in e-mail (M.A. More): mam@physics.unipune.ac.in

The ZnO nanostructures were characterized by x-ray diffractometer (XRD; Model-D8, Advance, Bruker AXS) with Cu K $\alpha$  radiation ( $\lambda=1.5406 \text{ \AA}$ ), scanning electron microscope (SEM; JEOL, JSM-6360A) with the operating voltage of 20 kV and the emission current  $\sim 60 \mu\text{A}$ . The elemental composition was obtained by energy-dispersive x-ray spectrometer (EDS) attached to the SEM. For EDS studies, four 'spots' (area  $\sim 25 \mu\text{m}^2$ , each) at different locations on the sample were analyzed with data collection time of 80 seconds. Field emission current versus applied voltage (I-V) and current versus time (I-t) measurements were performed in a planar diode configuration at a base pressure of  $\sim 1.0 \times 10^{-8}$  mbar. The details of the field emission system and experimental methodology are given elsewhere [15]. In brief, the annealed Au coated Zn foil (i.e. the ZnO nanostructured thin film) served as a cathode and a semi-transparent phosphor screen as an anode. The cathode-anode assembly was held parallel to each other with separation of  $\sim 1 \text{ mm}$ . The field emission current was measured at room temperature using Keithley 485 Picoammeter and a Spellman high voltage DC power supply (0-40 kV, Spellman, USA). A care was taken to avoid any leakage current using shielded cables with proper grounding.

### III. RESULTS AND DISCUSSION

The X-ray diffraction (XRD) patterns of the samples annealed at 300 °C and 400 °C are shown in Fig. 1. The XRD patterns exhibit a set of well defined diffraction peaks indicating formation of polycrystalline phases. The peaks are indexed to the hexagonal wurtzite ZnO structure. In addition, some peaks corresponding to metallic Au and Au-Zn alloy have been observed. The disappearance of diffraction peak corresponding to Au, when the annealing is carried out at 400 °C and simultaneous appearance of more diffraction corresponding to Au-Zn phases indicates that the growth rate is higher at higher annealing temperature.

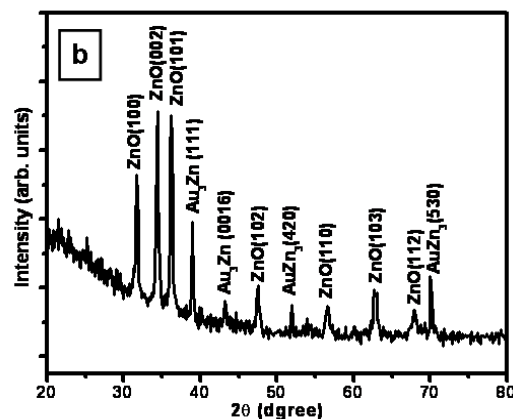
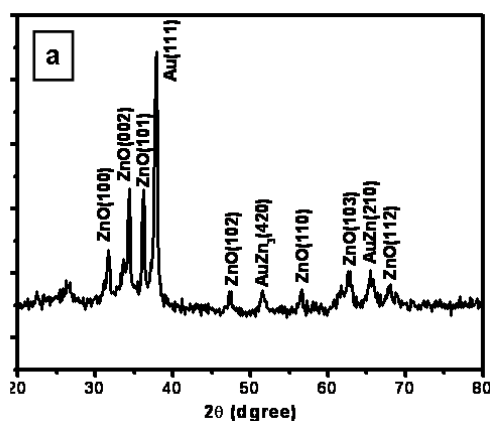


Fig. 1 XRD patterns of the specimen annealed at (a) 300 °C and (b) 400 °C for 4 hour in air.

Fig. 2 and 3 show typical SEM images of the samples annealed at 300 °C and 400 °C for 4 hours in the air, respectively. As revealed from the SEM images, growth of ZnO nanostructures is observed to occur mainly on the gold islands. It indicates the catalytic role of the gold particles during growth of the ZnO nanostructures, as reported in the literature [8]. The SEM images depict that the overall surface roughness is more, when the annealing carried out at higher temperature i.e. 400 °C.

The ZnO nanowires show slight tapering from the base to top. A careful observation of the SEM images indicate that although the ZnO nanowires are nearly aligned in each case, their areal density is seen to be higher when the annealing is carried out at higher temperature i.e. at 400 °C. From the high magnification SEM images the diameter and length of these wires are found to be in the range of few nano meters and several microns, respectively. However, the nanowires obtained at higher annealing temperature are seen to possess high aspect ratio.

Formation of the ZnO nanowires exclusively on the gold islands is as per the vapour-solid-solid (VSS) mechanism, explained in detail elsewhere [8]. In short, during the annealing in air, the Zn atoms undergo solid-phase diffusion from substrate (zinc foil) to the surface, which form Au-Zn alloy particles. The Au/Au-Zn alloy particles play catalytic role in the growth of the ZnO nanowires, first acting as nucleation sites and then initiating the growth process.

The chemical composition of the annealed samples, obtained from the EDS spectra show presence of Zn, O and Au only. No peaks corresponding to other materials are observed, indicating the chemical purity of the samples.

The J-E characteristic of the samples annealed at 300 °C and 400 °C is depicted in Fig. 3. The turn-on field corresponding to emission current density of  $10 \mu\text{A}$  is found to be  $1.20 \text{ V}/\mu\text{m}$  and  $2.92 \text{ V}/\mu\text{m}$  for the sample annealed at

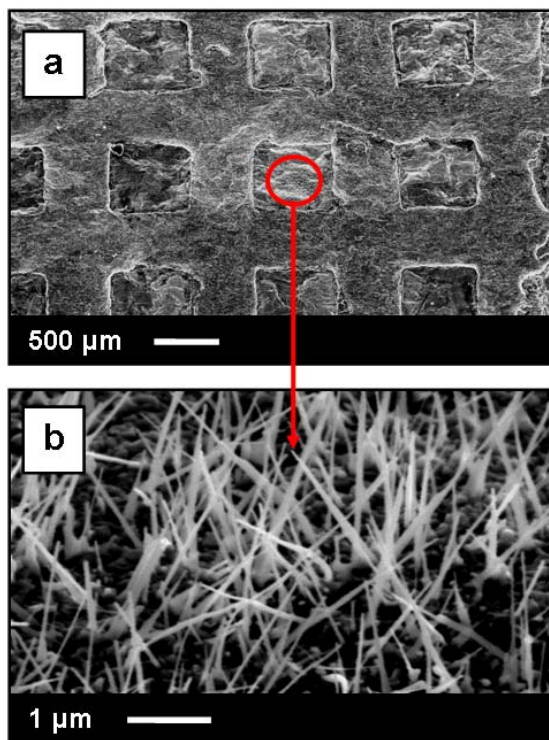


Fig. 2 (a and b) The top-view SEM images of the patterned Au coated on zinc foil after annealing at 300 °C for 4 hour in air.

300 °C and 400 °C, respectively. As the applied voltage is increased, the emission current is observed to increase rapidly and emission current density of  $\sim 425 \mu\text{A}/\text{cm}^2$  and  $185 \mu\text{A}/\text{cm}^2$ , has been drawn from the samples annealed at 300 °C and 400 °C at applied field of  $\sim 2.8 \text{ V}/\mu\text{m}$  and  $3.96 \text{ V}/\mu\text{m}$ , respectively. For the sake of comparison with other results reported in the literature, the threshold field, required to draw emission current density  $\sim 100 \mu\text{A}/\text{cm}^2$ , is observed to be  $1.70 \text{ V}/\mu\text{m}$  and  $3.74 \text{ V}/\mu\text{m}$  for the specimen annealed at 300 °C and 400 °C, respectively. The observed values of turn-on and/or threshold field are comparable to those reported for various ZnO nanostructures [4-7]. It is well known, there are several factors which can effect the value of turn-on field such as shape (aspect ratio/tip radius), crystallinity, conductivity, effective work function and areal density of the emitters. As seen from the SEM results the sample annealed at 400 °C possess higher areal density of nanowires. The higher emitter density is expected to cause stronger field screening effect which in turn will lead to enhancement in the turn on field value.

In the present studies, the current density ( $J$ ) is estimated by considering the entire area of the emitter and defined as  $J = I/A$ , where  $I$  is the measured emission current and  $A$  is the total area of the emitter. The applied field ( $E$ ) is defined as  $E = V/d$ , where  $V$  is the applied voltage and  $d$  is the separation between the emitter cathode and the anode. This field is also referred to as an “average field”.

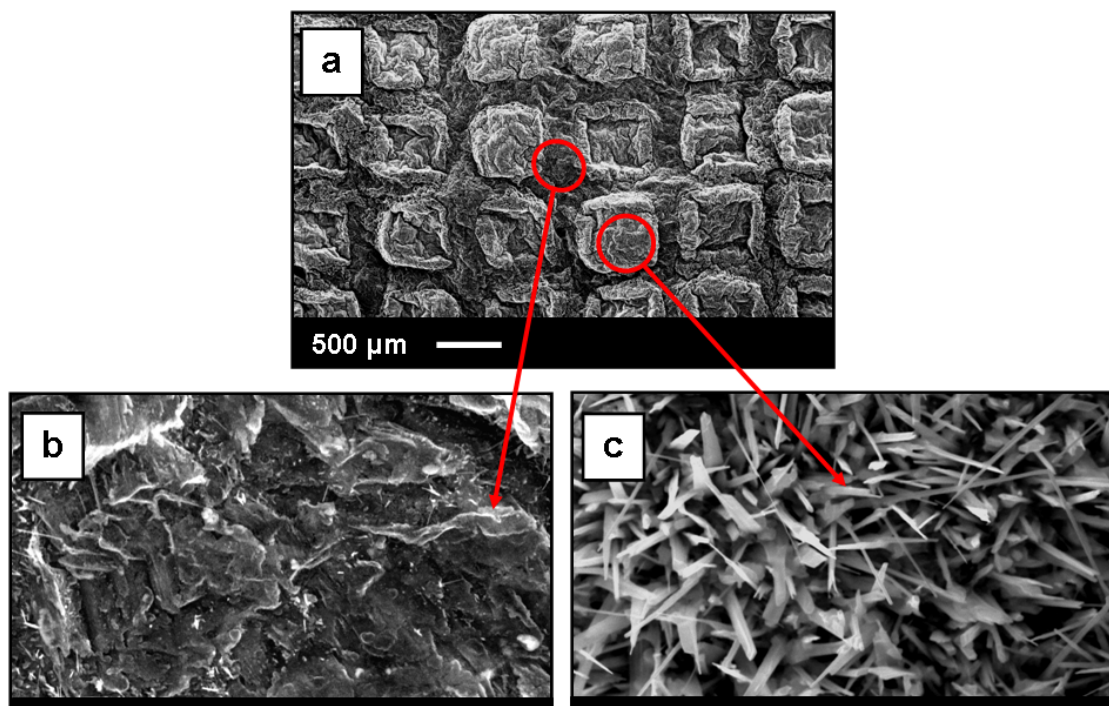


Fig. 3 (a) The top-view SEM images of the patterned Au coated on zinc foil after annealing at 400 °C for 4 hour in air. The high magnification SEM images of the sample (b) between and (c) within the squares (patterned).

The emission current density versus applied field (J-E) characteristics were analyzed by the Fowler–Nordheim (F–N) equation [16]

$$J = A (\beta^2 E^2 / \phi) \exp(-B\phi^{3/2} / \beta E) \quad (1)$$

where, J is the emission current density, A ( $1.54 \times 10^{-6}$  A eV/V<sup>2</sup>) and B ( $6.83 \times 10^9$  eV<sup>-3/2</sup> V/m) are constants,  $\phi$  is the work function and  $\beta$  is field enhancement factor.

The Fowler-Nordheim (F-N) plot, i.e.  $\ln(J/E^2)$  versus  $(1/E)$ , derived from the observed J-E characteristic is shown as the insets in Fig. 4. The F-N plots show a nonlinear behaviour due to the fact that the patterned ZnO nanowires are semiconducting in nature. It is expected that the F-N plot for semiconducting emitter will show a non-linear behaviour, provided the I-V measurements are carried out in sufficiently high field range.

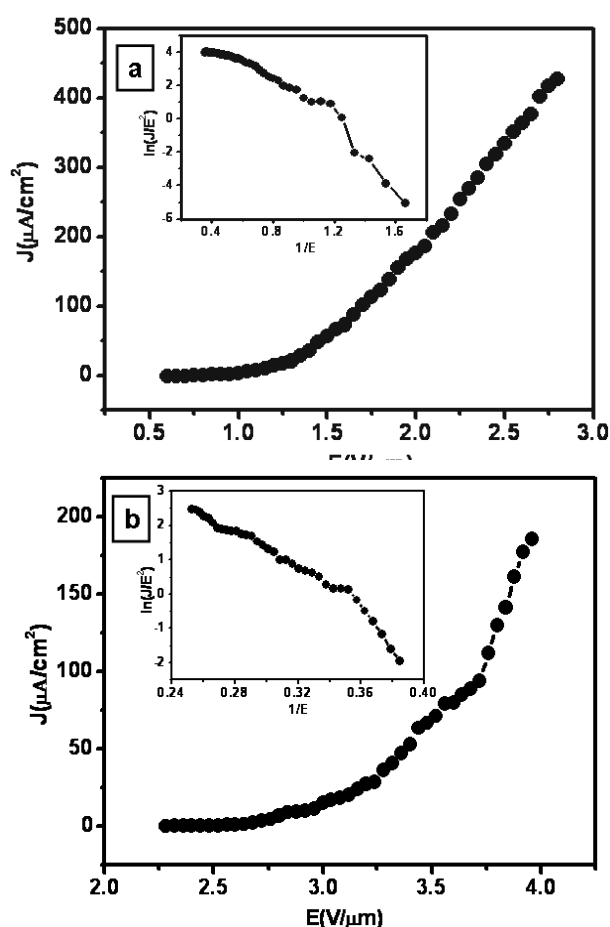
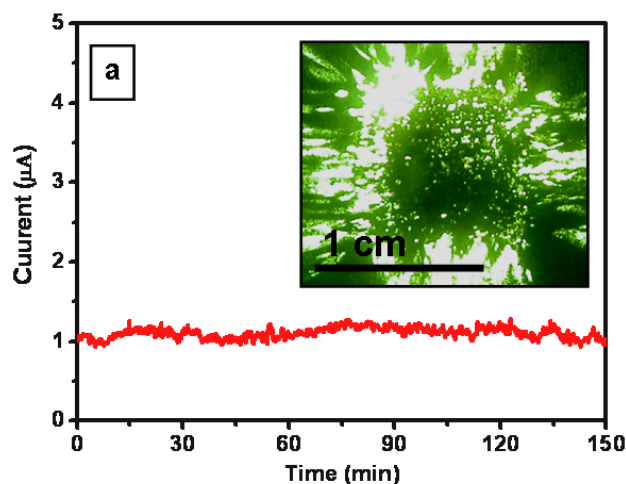


Fig. 4 (a) and (b) Field emission current density versus applied field (J-E) of samples annealed at 300 °C and 400 °C for 4 hour in air, respectively. The insets show the corresponding Fowler-Nordheim (F-N) plots.

The emission current stability of the annealed samples (emitters) have been investigated at the pre-set current value

of 1  $\mu\text{A}$  over the duration of 2.5 hours and the corresponding emission current-time (I-t) plots recorded at the base pressure of  $1 \times 10^{-8}$  mbar are shown in Fig. 4. As seen from Fig. 4, the specimen annealed at 300 °C and 400 °C show good emission stability at the pre-set current value. The emission current exhibits excursions from the average value along with some superimposed ‘spike’-type fluctuations. The ‘spike’-type fluctuations are due to the adsorption, desorption and/or migration of the residual gas molecules on the emitter surface. The variations in the emission current can be understood by the role played by the residual gas ion bombardment during the continuous operation of the emitter. There are various processes occurring simultaneously on the emitter surface which affect the emission current. Since we have used as prepared samples for field emission studies, it is expected that the emitter surface is “not clean”. As no cleaning attempt such as degassing by heating the emitter has been carried out it is expected that there will be more adsorbed gas trapped into the voids between the nanostructures which will slowly emerge during the ion bombardment. The trend in the observed I-t curve is indicative of the ion bombardment induced cleaning of the emitter surface. The results suggest that the patterned ZnO nanowires emitter is a potentially important system for applications in field emission based devices. A post field emission SEM study indicated no significant change in the overall surface morphology of ZnO nanowires emphasizing that the nanowires are mechanically robust against the stress due to the intense applied electric field and ion bombardment. Typical field emission images, captured at current value of 10  $\mu\text{A}$  are shown as inset of Fig. 4. The images show the number of tiny spots, which correspond to emission from the most protruding ZnO nanowires (annealed samples). Temporal changes in the image spots intensity have been observed to be commensurate with the emission current fluctuation as seen in I-t plot.



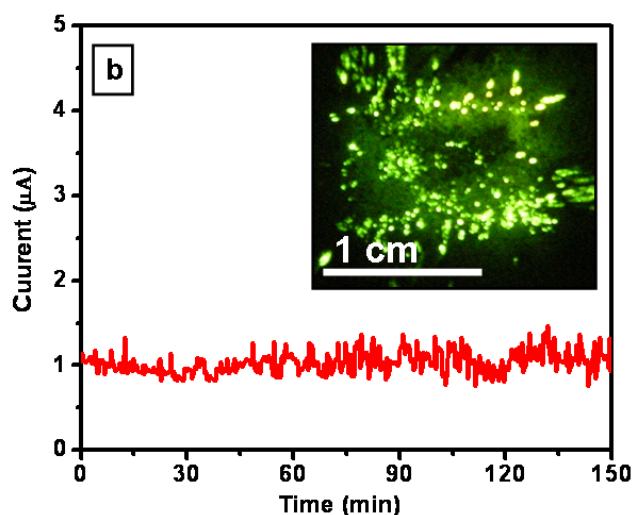


Fig. 5 (a) and (b) Field emission current stability (I-t) plots of the samples annealed at 300 °C and 400 °C for 4 hours in air for 2.5 hours duration, respectively. The insets show typical field emission images recorded at emission current density of  $\sim 10 \mu\text{A}/\text{cm}^2$  at the base pressure of  $\sim 1 \times 10^{-8}$  mbar.

#### IV. CONCLUSION

In summary, the patterned ZnO nanowire arrays were synthesized on zinc foil using a simple method, which combined photolithographic process with the thermal oxidation methods. The morphological studies show the length of ZnO nanowires are in the range of several microns with the average of diameter less than 500 nm. It is also found that the ZnO nanowires are not grown directly without using the gold layer. The field emission measurement reveal that the turn-on field required to draw emission current density of  $10 \mu\text{A}/\text{cm}^2$  and  $100 \mu\text{A}/\text{cm}^2$  are observed to be  $1.20 \text{ V}/\mu\text{m}$  and  $1.70 \text{ V}/\mu\text{m}$  for the sample annealed at  $300 \text{ }^\circ\text{C}$  and  $2.92 \text{ V}/\mu\text{m}$  and  $3.74 \text{ V}/\mu\text{m}$  for the annealed at  $400 \text{ }^\circ\text{C}$ , respectively. The emission current stability investigated at the preset value of  $\sim 1 \mu\text{A}$  is observed to be promising. The experimental results demonstrate that this technique can be significantly a promising method for making field emission based devices.

#### ACKNOWLEDGMENT

M.A.M would like to thank to CNQS. The field emission work has been carried out as a part of the CNQS (UPE-UGC programme) activity.

#### REFERENCES

- [1] L. Liao, H. B. Lu, J. C. Li, H. He, D. F. Wang, D. J. Fu, C. Liu, W. F. Zhang, *J. Phys. Chem. C* 111(2007)1900.
- [2] S. P. Lau, H. Y. Yang, S. F. Yu, H. D. Li, M. Tanemura, T. Okita, H. Hatano, H. H. Hng, *Appl. Phys. Lett.* 87(2005) 013104.
- [3] Z. L. Wang, *Materials Today*, 10 (2007) 20.
- [4] F. Jamali Sheini, D. S. Joag M. A. More, *Ultramicroscopy* 109 (2009) 418.
- [5] B. Cao, X. Teng, S. H. Heo, Y. Li, S. O. Cho, G. Li, W. Cai, *J. Phys. Chem. C* 111 (2007) 2470.
- [6] A. Wei, X. W. Sun, C. X. Xu, Z. L. Dong, M. B. Yu, W. Huang, *Appl. Phys. Lett.* 88 (2006) 213102.
- [7] D. Pradhan, M. Kumar, Y. Ando, K. T. Leung, *ACS Appl. Mater. Interfaces.* (2009) 789.
- [8] F. Jamali Sheini, D. S. Joag M. A. More, Jai Singh, O.N. Srivastava, *Materials Chemistry and Physics* 109 (2009) 418.
- [9] A. Umar, B. Karunakaran, S. H. Kim, E. -K. Suh, Y. B. Hahn, *Inorg. Chem.* 47 (2008) 4088.
- [10] H. Chik, J. Liang, S. G. Cloutier, N. Kouklin, J. M. Xu, *Appl. Phys. Lett.* 84 (2004) 3376.
- [11] Y. Wu, P. Yang, *J. Am. Chem. Soc.* 123 (2001) 3165.
- [12] X. Duan, C. M. Lieber *J. Am. Chem. Soc.* 122 (2000) 188.
- [13] Y. Zhang, K. Yu, S. Ouyang, Z. Zhu, *Mater. Lett.* 60 (2006) 522.
- [14] N. Liu, G. Fang, W. Zeng, H. Long, L. Yuan, X. Zhao, *Appl. Phys. Lett.* 95 (2009) 153505.
- [15] N. S. Ramgir, D. J. Late, A. B. Bhise, I. S. Mulla, M. A. More, D. S. Joag, V. K. Pillai, *Nanotechnology* 17 (2006) 2730.
- [16] R. H. Fowler, L. W. Nordheim, *Proc. R. Soc. London, Ser. A* 119 (1928) 173.